arXiv:astro-ph/0609463v2 5 May 2007

Cosmological neutrino mass limit and the dynamics of dark energy

Jun-Qing Xia, Gong-Bo Zhao and Xinmin Zhang
Institute of High Energy Physics, Chinese Academy of Science, P.O. Box 918-4, Beijing 100049, P. R. China

(Dated: February 5, 2008)

We investigate the correlation between the neutrino mass limit and dark energy with time evolving equation of state. Parameterizing dark energy as $w = w_0 + w_1 * z/(1+z)$, we make a global fit using Markov Chain Monte Carlo technique to determine w_0, w_1, neutrino mass as well as other cosmological parameters simultaneously. We pay particular attention to the correlation between neutrino mass Σm_ν and w_1 using current cosmological observations as well as the future simulated datasets such as PLANCK, SNAP and LAMOST.

I. INTRODUCTION

With the accumulation of high quality observational data of cosmic microwave background (CMB) [1, 2], large scale structure (LSS) of galaxies [3, 4, 5] and Supernovae Type Ia (SN Ia) [6, 7, 8], we have been pacing into a new era of precision cosmology. In 1998, the analysis of the luminosity-redshift relation of SN Ia revealed the current acceleration of our universe [9, 10]. This acceleration attributes to a new form of energy, dubbed dark energy (DE), with negative pressure and almost not clustering whose nature remains unveiled. The simplest candidate of dark energy is the cosmological constant (CC) however it suffers from the fine tunning and coincidence problems [11, 12]. To ameliorate these dilemmas some dynamical dark energy models such as quintessence [13], phantom [14], k-essence [15] and quintom whose equation of state (EOS) can cross -1 during evolution [16] have been proposed and studied thoroughly both theoretically and phenomenologically in the literature [16, 17, 18, 19, 20, 21, 22, 23, 24, 25, 26, 27, 28, 29].

Neutrino physics, especially the mass limit, is another challenge of modern science. The combined analysis of all currently available data of neutrino oscillation experiments implies the crucial mass differences in the neutrino mass hierarchy, say, $\Delta m^2_{12} \simeq 7 \times 10^{-5}\mathrm{eV}^2$, $\Delta m^2_{23} \simeq 2.6 \times 10^{-3}\mathrm{eV}^2$ for solar neutrino and the atmospheric neutrino mass difference respectively [30]. In the scenario of hierarchical neutrino masses these results suggest $m_1 \sim 0$, $m_2 \sim \Delta m_{\mathrm{solar}}$, and $m_3 \sim \Delta m_{\mathrm{atmospheric}}$. For the inverted hierarchy $m_3 \sim 0$, $m_2 \sim \Delta m_{\mathrm{atmospheric}}$, and $m_1 \sim \Delta m_{\mathrm{atmospheric}}$. However, if the neutrino masses are degenerate, one finds $m_1 \sim m_2 \sim m_3 \gg \Delta m_{\mathrm{atmospheric}}$. These oscillation experiments can merely constrain the squared mass differences, Δm^2, they cannot detect the absolute value of neutrino masses which is of great significance.

However, cosmological observations can put upper limits of the absolute neutrino mass. For background evolution, neutrino masses contribute to the cosmic energy budget so that modify the epoch of matter-radiation equality, angular diameter distance to the last scattering surface (LSS) and other related physical quantities. For the perturbation, neutrinos become non-relativistic at late time thus they damp the perturbation within their free streaming scale. This suppressed the matter power spectrum by roughly $\Delta P/P \sim -8\Omega_\nu/\Omega_m$ [31]. Dark energy can also affect the evolution of background and perturbation, which can mimic the behavior of neutrino to some extent, so that there exists an obvious correlation between equation of state of dark energy and neutrino mass.

For simplicity, Ref.[32, 33] parameterizes dark energy by constant equation of state and finds it strongly correlates with neutrino mass. In this paper, we study this correlation with dynamical dark energy models which are more generic with current cosmological observations as well as with future simulated data. Further we have determined the parameters of dynamical dark energy and neutrino mass limit simultaneously.

The rest part of this paper is structured as follows: in the next section we present our fitting method and data we use. In section III we give our results. We make conclusion and discussion in the last section.

II. METHOD AND DATA

We choose the commonly used parametrization of the EOS of dark energy as [34]:

$$w(z) = w_0 + w_1 \frac{z}{1+z} , \tag{1}$$

where z is the redshift. Clearly the cosmological constant corresponds to $w_0 = -1$, $w_1 = 0$ thus ΛCDM model is incorporated in this parametrization. For neutrino mass, we use the parameter f_ν which is defined as dark matter neutrino fraction:

$$f_\nu = \rho_\nu/\rho_{DM} = \frac{\Sigma m_\nu}{93.105\ eV\ \Omega_c h^2} , \tag{2}$$

where ρ_ν and ρ_{DM} denote the energy density of neutrino and dark matter respectively, Σm_ν is the sum of neutrino mass and $\Omega_c h^2$ is the physical cold dark matter densities relative to critical density.

The fitting and statistics strategy we adopt is based on the Markov Chain Monte Carlo package `CosmoMC` [35][1], which has been modified to implement dark energy perturbations with EOS getting across -1 [19]. Our most general parameter space is

$$\mathbf{p} \equiv (\omega_b, \omega_c, \Theta_S, \tau, w_0, w_1, f_\nu, n_s, \log[10^{10}A_s]) \ , \tag{3}$$

where $\omega_b = \Omega_b h^2$ and $\omega_c = \Omega_c h^2$ are the physical baryon and cold dark matter densities relative to critical density, Θ_S is the ratio (multiplied by 100) of the sound horizon to the angular diameter distance at decoupling, τ is the optical depth, A_s is defined as the amplitude of initial power spectrum and n_s measures the spectral index. Assuming a **flat** Universe motivated by inflation and basing on the Bayesian analysis, we vary the 9 parameters above and fit to the observational data with the MCMC method. We take the weak priors as: $\tau < 0.8, 0.5 < n_s < 1.5, -3 < w_0 < 3, -5 < w_1 < 5$ [2]$, 0 < f_\nu < 0.5$ and a cosmic age tophat prior as 10 Gyr< t_0 <20 Gyr. Furthermore, we make use of the HST measurement of the Hubble parameter $H_0 = 100h$ km s^{-1}Mpc^{-1} [36] by multiplying the likelihood by a Gaussian likelihood function centered around $h = 0.72$ and with a standard deviation $\sigma = 0.08$. We impose a weak Gaussian prior on the baryon density $\Omega_b h^2 = 0.022 \pm 0.002$ (1σ) from Big Bang nucleosynthesis [37].

In our global fitting we compute the total likelihood to be the products of separate likelihoods of CMB, SNIa, LSS and Heidelberg-Moscow experiment (HM) [38, 39, 40]. Alternatively defining $\chi^2 = -2\log\mathcal{L}$, so

$$\chi^2_{total} = \chi^2_{CMB} + \chi^2_{SNIa} + \chi^2_{LSS} + \chi^2_{HM} \ . \tag{4}$$

For CMB data we use the three-year WMAP (WMAP3) Temperature-Temperature (TT) and Temperature-Polarization (TE) power spectrum with the routine for computing the likelihood supplied by the WMAP team [41]. The supernova data we use are the "gold" set of 157 SNIa published by Riess *et al* in [7]. We have marginalized over the nuisance parameter [42] in the calculation of SN Ia likelihood. For LSS information, we have used the 3-D matter power spectrum of SDSS [4] and 2dFGRS [3], Lyman-α forest data (Lyα) from SDSS [43] and recent measurement of the baryon acoustic oscillation feature in the 2-point correlation function of SDSS [44]. To be conservative but more robust, we only use the first 14 bins of the SDSS 3-D matter power spectrum, which are well within the linear regime [45]. For Lyα likelihood, we modify the interpolating code[3] to incorporate dynamical dark energy models. For BAO likelihood, we use the constraint[4] [44]:

$$A \equiv D_V(0.35)\frac{\sqrt{\Omega_m H_0^2}}{0.35c} = 0.469 \pm 0.017 \ , \tag{5}$$

$$D_V(z) = \left[D_M(z)^2 \frac{cz}{H(z)}\right]^{1/3} \ , \tag{6}$$

where $H(z)$ is the Hubble parameter, c is the speed of light and $D_M(z)$ is the comoving angular diameter distance at a specific redshift z. Thus

$$\chi^2_{BAO} = \frac{(A - 0.469)^2}{0.017^2} \ . \tag{7}$$

Moreover, the Heidelberg-Moscow experiment uses the half time of $0\nu2\beta$ decay to constrain the effective Majorana mass and this translates to the constraints of sum of neutrino mass under some assumptions [47]:

$$\Sigma m_\nu \sim 1.8 \pm 0.6eV \ (2\sigma) \ . \tag{8}$$

---

[1] Available at http://cosmologist.info/cosmomc/

[2] We set the prior of w_0 and w_1 broad enough to ensure the EoS can evolve in the whole parameter space.

[3] Available at http://www.cita.utoronto.ca∼pmcdonal/LyaF/public.lyafchisq.tar.gz

[4] In this work we mainly focus on the correlation between dark energy parameters and the neutrino mass rather than the absolute value of the neutrino mass. What we are interested in is the possible effect of BAO measurement on this correlation. Since the BAO measurement seems not very consistent with the other observations, such as CMB and SN Ia, on the constraints of dark energy parameters, we don't use the full power spectrum analysis of BAO in our calculations for simplicity. Similarly the author of Ref.[46] also use the parameter A to study the neutrino mass limit.

Given the Heidelberg-Moscow experiment is controversial for the time being and seems not consistent with other observational data, we just make a tentative fit choosing the HM prior to illustrate the effect on the correlation between the dark energy parameters and the neutrino mass when the total neutrino mass is very large.

To get robust conclusion, we have also used the simulated data from future observations of PLANCK, LAMOST and SNAP. The fiducial model we choose is the best-fit from the WMAP3 dataset [1]: $\Omega_b = 0.04$, $\Omega_c = 0.20$, $h_0 = 0.73$, $\tau = 0.088$, $n_s = 0.95$ and $A_s = 0.68$. And we assume the sum of neutrino mass $\sum m_\nu = 0$ and the equation of state of dark energy $w_0 = -1$, $w_1 = 0$.

For the CMB simulation we consider a simple full-sky ($f_{sky} = 1$) simulation at Planck-like sensitivity and ignore the lensing effect and the tensor information. We neglect foregrounds and assume the isotropic noise with variance $N_l^{TT} = N_l^{EE}/2 = 3 \times 10^{-4} \mu K^2$ (Pessimistic Planck-like sensitivity) and a symmetric Gaussian beam of 7 arcminutes full-width half-maximum (FWHM) [48]. We use the simulated $\tilde{C}_l$ up to $l = 2500$ for temperature and $l = 1500$ for polarization. The effective χ^2 is:

$$\chi^2_{eff} \equiv -2\log\mathcal{L} = \sum_l (2l+1)\left\{\log\left(\frac{C_l^{TT}C_l^{EE}-(C_l^{TE})^2}{\tilde{C}_l^{TT}\tilde{C}_l^{EE}-(\tilde{C}_l^{TE})^2}\right) + \frac{\tilde{C}_l^{TT}C_l^{EE}+C_l^{TT}\tilde{C}_l^{EE}-2\tilde{C}_l^{TE}C_l^{TE}}{C_l^{TT}C_l^{EE}-(C_l^{TE})^2} - 2\right\} , \tag{9}$$

where C_l^{XY} denote theoretical power spectra and $\tilde{C}_l^{XY}$ denote the power spectra from the simulated data. The likelihood has been normalized with respect to the maximum likelihood, where $C_l^{XY} = \tilde{C}_l^{XY}$ [49, 50].

For the future LSS survey we consider LAMOST project. The Large Sky Area Multi-Object Fiber Spectroscopic Telescope (LAMOST) project as one of the National Major Scientific Projects undertaken by the Chinese Academy of Science, aims to measure $\sim 10^7$ galaxies with mean redshift $z \sim 0.2$ [51]. In the measurements of large scale matter power spectrum of galaxies there are generally two statistical errors: sample variance and shot noise. The uncertainty due to statistical effects, averaged over a radial bin Δk in Fourier space, is [52]

$$(\frac{\sigma_P}{P})^2 = 2 \times \frac{(2\pi)^3}{V} \times \frac{1}{4\pi k^2 \Delta k} \times (1 + \frac{1}{\bar{n}P})^2 . \tag{10}$$

The initial factor of 2 is due to the real property of the density field, V is the survey volume and $\bar{n}$ is the mean galaxy density. In our simulations for simplicity and to be conservative, we use only the linear matter power spectrum up to $k \sim 0.1\ h\ \mathrm{Mpc}^{-1}$.

The projected satellite SNAP[5] (Supernova / Acceleration Probe)would be a space based telescope with a one square degree field of view with 1 billion pixels. It aims to increase the discovery rate for SNIa to about 2,000 per year [53]. The simulated SN Ia data distribution is taken from Refs.[54, 55]. As for the error, we follow Ref.[54] which takes the magnitude dispersion 0.15 and the systematic error $\sigma_{sys}(z) = 0.02 \times z/1.7$, and the whole error for each data is

$$\sigma_{mag}(z_i) = \sqrt{\sigma^2_{sys}(z_i) + \frac{0.15^2}{n_i}} , \tag{11}$$

where n_i is the number of supernova in the i'th redshift bin.

For each regular calculation, we run 6 independent chains comprising of 150,000-300,000 chain elements and spend thousands of CPU hours to calculate on a cluster. The average acceptance rate is about 40%. And for the convergence test typically we get the chains satisfy the Gelman and Rubin [56] criteria where R-1<0.1.

Despite our ignorance of the nature of dark energy, it is more natural to consider the DE fluctuation whether DE is regarded as scalar field or fluid rather than simply switching it off. The conservation law of energy reads:

$$T^{\mu\nu}{}_{;\mu} = 0 , \tag{12}$$

where $T^{\mu\nu}$ is the energy-momentum tensor of dark energy and ";" denotes the covariant differentiation. Working in the conformal Newtonian gauge, Equation(12) leads to the perturbation equations of dark energy as follows [57]:

$$\dot{\delta} = -(1+w)(\theta - 3\dot{\Phi}) - 3\mathcal{H}(\delta p/\delta\rho - w)\delta , \tag{13}$$

$$\dot{\theta} = -\mathcal{H}(1-3w)\theta - \frac{\dot{w}}{1+w}\theta + k^2(\frac{\delta p/\delta\rho}{1+w}\delta + \Psi) . \tag{14}$$

---

[5] SNAP is one of the several candidates emission concepts for the Joint Dark Energy Mission(JDEM).

TABLE 1. Median values and 1σ constrains on dark energy parameters and sum of neutrino mass for models discussed in the text. From left to right, we use WMAP three year data (WMAP3), WMAP3+Riess 157 “Gold” sample+2dF+SDSS(14bands)(LSS), WMAP3+LSS+Lyman-α forest(Lyα), WMAP3+LSS+Lyman-α+Baryon Acoustic Oscillation (BAO) information, WMAP3+LSS+Lyα+BAO+Heidelberg-Moscow experiment data respectively. The right most column we use the simulated data for future SNAP+PLANCK+LAMOST. For one-tailed distributed parameter such as neutrino mass, we quote the 95% C.L. limit.

	m_ν+Dynamical Dark Energy with Dark Energy Perturbation					
	WMAP3	+SN+LSS	+Lyα	+BAO	+Heidelberg-Moscow	Planck+SNAP+LAMOST
w_0	$-1.004^{+0.662}_{-0.717}$	$-1.212^{+0.228}_{-0.209}$	$-1.138^{+0.196}_{-0.204}$	$-0.820^{+0.219}_{-0.214}$	$-0.725^{+0.277}_{-0.252}$	$-0.984^{+0.070}_{-0.069}$
w_1	$-1.939^{+2.459}_{-2.098}$	$0.418^{+0.823}_{-0.848}$	$0.125^{+0.859}_{-0.842}$	$-0.924^{+1.077}_{-1.095}$	$-1.894^{+1.472}_{-1.651}$	$-0.173^{+0.266}_{-0.278}$
$\Sigma m_\nu(eV)$	< 4.532	< 2.896	< 1.149	< 0.490	$0.971^{+0.225}_{-0.239}$	< 0.323
$cov(w_0, m_\nu)$	-0.067	-0.382	-0.221	0.110	0.086	0.0005
$cov(w_1, m_\nu)$	-0.077	-0.109	-0.117	-0.171	-0.170	-0.295

	m_ν+Dynamical Dark Energy without Dark Energy Perturbation					
	WMAP3	+SN+LSS	+Lyα	+BAO	+Heidelberg-Moscow	Planck+SNAP+LAMOST
w_0	$-0.859^{+0.564}_{-0.558}$	$-1.174^{+0.181}_{-0.180}$	$-1.170^{+0.173}_{-0.170}$	$-0.901^{+0.147}_{-0.155}$	$-0.846^{+0.180}_{-0.179}$	–
w_1	$-0.571^{+1.342}_{-1.365}$	$0.393^{+0.555}_{-0.553}$	$0.440^{+0.567}_{-0.560}$	$-0.342^{+0.595}_{-0.585}$	$-0.960^{+0.868}_{-0.915}$	–
$\Sigma m_\nu(eV)$	< 4.684	< 2.786	< 0.991	< 0.433	$0.899^{+0.247}_{-0.244}$	–
$cov(w_0, m_\nu)$	0.041	-0.447	-0.295	0.013	0.089	–
$cov(w_1, m_\nu)$	-0.143	-0.017	0.023	-0.131	-0.236	–

	m_ν+WCDM with Dark Energy Perturbation					
	WMAP3	+SN+LSS	+Lyα	+BAO	+Heidelberg-Moscow	Planck+SNAP+LAMOST
w	–	–	–	$-0.978^{+0.071}_{-0.066}$	–	–
$\Sigma m_\nu(eV)$	–	–	–	< 0.398	–	–
$cov(w, m_\nu)$	–	–	–	-0.137	–	–

	m_ν+ΛCDM					
	WMAP3	+SN+LSS	+Lyα	+BAO	+Heidelberg-Moscow	Planck+SNAP+LAMOST
$\Sigma m_\nu(eV)$	–	–	< 0.299	–	–	–

For the models where the EOS doesn’t cross -1, the above equation(13), (14) is well defined. For the crossing models, the perturbation equation (13), (14) is seemingly divergent. However basing on the realistic two-field-quintom model as well as the single field case with a high derivative term [19], the perturbation of DE is shown to be continuous when the EOS gets across -1, thus we introduce a small positive parameter ϵ to divide the full range of the allowed value of the EOS w into three parts: 1) $w > -1 + \epsilon$; 2) $-1 + \epsilon \geq w \geq -1 - \epsilon$; and 3) $w < -1 - \epsilon$.

For the regions 1) and 3) the perturbation is well defined by solving Eqs.(13), (14) as shown above. For the case 2), the perturbation of energy density δ and divergence of velocity, θ, and the time derivatives of δ and θ are finite and continuous for the realistic quintom dark energy models. However for the perturbations with the above parameterizations clearly there exists some divergence. To eliminate the divergence typically one needs to base on the multi-component DE models which result in the non-practical parameter-doubling. A simple way out is to match the perturbation in region 2) to the regions 1) and 3) at the boundary and set [19, 20, 21]

$$\dot{\delta} = 0 \quad , \quad \dot{\theta} = 0 \; . \tag{15}$$

We have numerically checked the error in the range $|\Delta w = \epsilon| < 10^{-5}$ and found it less than 0.001% to the exact multi-field quintom model. Therefore our matching strategy is a perfect approximation to calculate the perturbation consistently for crossing models. For more details of this method we refer the readers to our previous companion papers [19, 20, 21].

III. RESULTS

In this section we present our global fitting results of dark energy parameters w_0, w_1 and neutrino mass limit. We pay particular attention to the correlation between w_1, which delineates the time evolving of dark energy, and neutrino mass. Our main result was summarized in Table I. We choose the general model of 9 free parameters as illustrated in Eq.(3) to study the correlation between dynamical dark energy and neutrino mass and discuss the model with DE with constant equation of state (WCDM) and ΛCDM model for comparison. Here we only list the parameters of dark energy and neutrino mass. Since dark energy perturbation is crucial in determination of cosmological parameters especially for dark energy parameters [1, 19, 20, 22], we include the full dark energy perturbation in our global fitting as well as showing the result by incorrectly switching off dark energy perturbations to reinforce this key point. We use different data combination discussed in previous section. The cov(X,Y) is the correlation coefficient of samples which quantifies the correlation between the two parameters X and Y defined as[58]:

$$cov(X,Y)=\frac{\sum_{i=1}^{n}(X_i-\bar{X}_i)(Y_i-\bar{Y}_i)}{\sqrt{\sum_{i=1}^{n}(X_i-\bar{X}_i)^2}\sqrt{\sum_{i=1}^{n}(Y_i-\bar{Y}_i)^2}}\ , \tag{16}$$

where the bar denotes the mean value of parameters. If cov(X,Y)>0 means X,Y is positively correlated and *vice versa*.

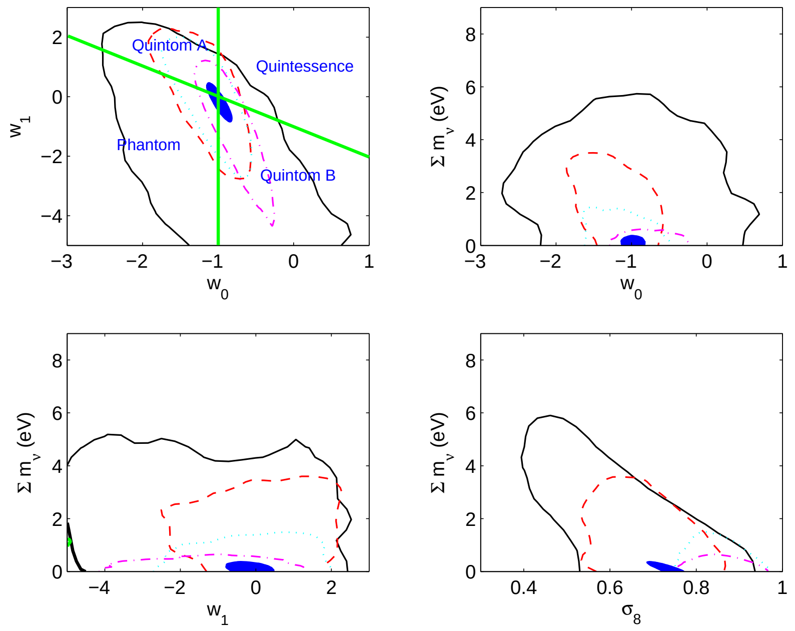

FIG. 1: 95% C.L.contour plots of the sum of neutrino mass Σm_ν with dark energy parameters w_0, w_1 as well as σ_8 with different combination of datasets. From outside in , we use WMAP3 only (black), WMAP3+RIESS+SDSS+2dF (red), WMAP3+RIESS+SDSS+2dF+Lyα (cyan), WMAP3+RIESS+SDSS+2dF+Lyα+BAO (purple) and simulated data of SNAP+PLANCK+LAMOST (innermost blue shaded). The two lines in the w_0, w_1 plane distinguish the dark energy models (see text) and their intersecting point denotes the ΛCDM model. In the fitting we include the full dark energy perturbations of dynamical dark energy models.

From the comparison of results with/without dark energy perturbation, we find dark energy perturbation modifies the mean value of all the parameters as well as enlarging the corresponding errors which is consistence with previous analysis in the literature [1, 19, 20, 22]. We will merely discuss the results with dark energy perturbation hereafter. We have seen that WMAP3 only put weak constraints on w_0, w_1 and neutrino mass since CMB data is sensitive to the effective equation of state of dark energy defined as [59]:

$$w_{eff}\equiv\frac{\int da\Omega(a)w(a)}{\int da\Omega(a)}\ , \tag{17}$$

thus it's hard to constrain w_0, w_1 and neutrino mass by CMB data alone. Adding SN Ia and LSS data we find the mean value of each parameter gets modified and the error bars shrink a lot. However it is noteworthy that adding BAO data enlarges the error of w_0, w_1 while tightens the neutrino mass limit to a great extent. If we take the HM prior in Eq.(8), we find the error of w_0, w_1 become greater while the 1-D posterior distribution of neutrino mass turns to be two-tailed. We have also done the global fitting using the simulated data of future observation and found the errors shrink greatly.

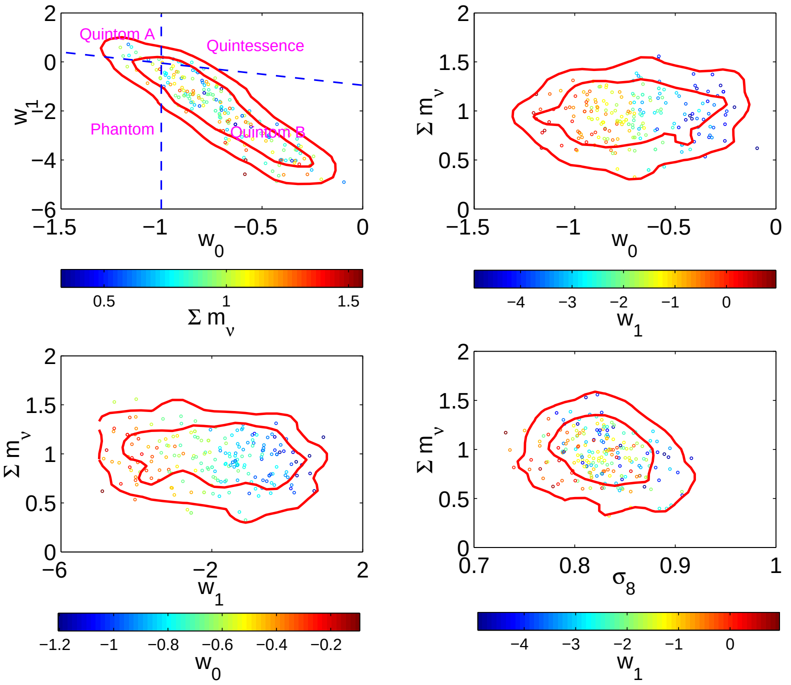

FIG. 2: 3-D scatter and 68% and 95% C.L. contour plots of the sum of neutrino mass Σm_ν with dark energy parameters w_0, w_1 as well as σ_8 using WMAP3+RIESS+SDSS+2dF+Lyman-α+BAO +Heidelberg-Moscow. Dark energy perturbation is also included.

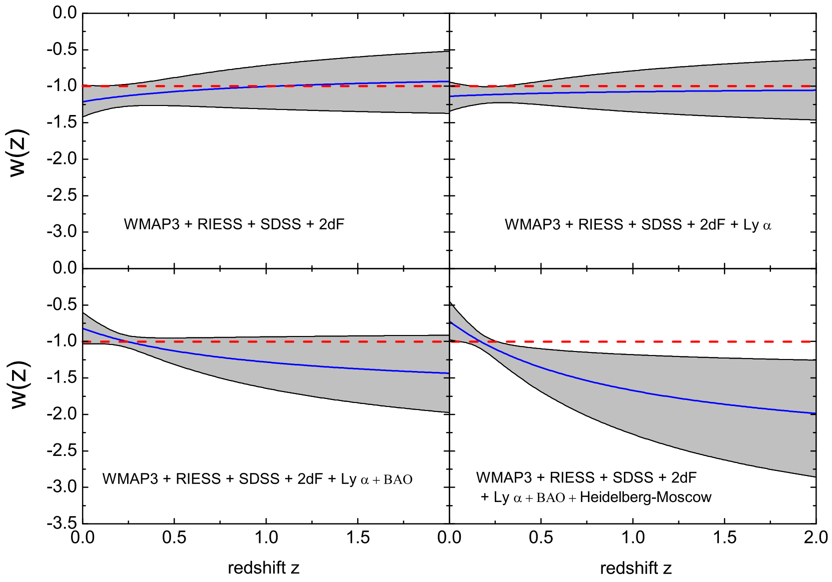

FIG. 3: Evolution of the equation of state of dark energy constrained by different combination of datasets as illustrated in the plots. The blue solid curve and the gray shaded bands show the mean value and 1-σ error respectively. Dark energy perturbation is fully included.

In Fig.(1) we show the 95% C.L. 2-D contours of w_0, w_1, neutrino mass and σ_8. From outside in, we add data as illustrated in the figure caption. Using simulated data we obtain the inner most shaded regions. The contours shrink significantly while interesting correlations remain. The results including HM prior are illustrated in Fig.(2). We also cut the $w_0 - w_1$ plane into four parts for different dark energy models as we did in [20, 21, 22]. The EOS of Quintom A crossing -1 from upside down, *i.e.* the EOS is greater than -1 in the early epoch yet negative than -1 currently while quintom B crosses -1 from the opposite direction. We find that the ΛCDM model cannot be ruled out by all the data combination at 2σ level however the quintom-like dynamical dark energy model is mildly favored. The one dimensional constraints of EOS by different combination of datasets are illustrated in Fig.(3). We find that the best fit models are always allowed crossing the boundary $w = -1$ in these four combinations. When adding the dataset of BAO measurement or HM measurement the direction of EOS crossing the boundary will be changed. This is due to the changed sign of the mean value of w_1. And the HM prior seems favor more negative value of w_1 and stronger evolution of EOS.

In Ref.[32], the author just used the constant EOS to consider the correlation between EOS of dark energy and neutrino mass. The critical point of our result is the correlation among w_0, w_1 and neutrino mass. From the table I we find there *exists* some correlation of $(w_0,\ m_\nu)$ and especially for w_1 and m_ν. More interestingly, we find using future high quality data, the correlation between w_0 and m_ν nearly vanishes while there is a strong and negative correlation between the "running" of dark energy EOS w_1 and the total neutrino mass Σm_ν. Fig.(4) delineates the fitting result of future simulation in more detail and we clearly see the strong correlations between w_1 and neutrino mass. In Ref.[60], the authors conclude w_1 is not strongly correlated with neutrino mass basing on Fisher matrix analysis. However, we have seen the distribution of w_1 and neutrino mass is highly non-Gaussian and Fisher matrix technique is not viable in such cases [50]. Furthermore, they didn't consider dark energy perturbation when EOS crosses -1. This also give rise to great bias of determining neutrino mass limit if neglecting time evolving of dark energy as illustrated in the table I.

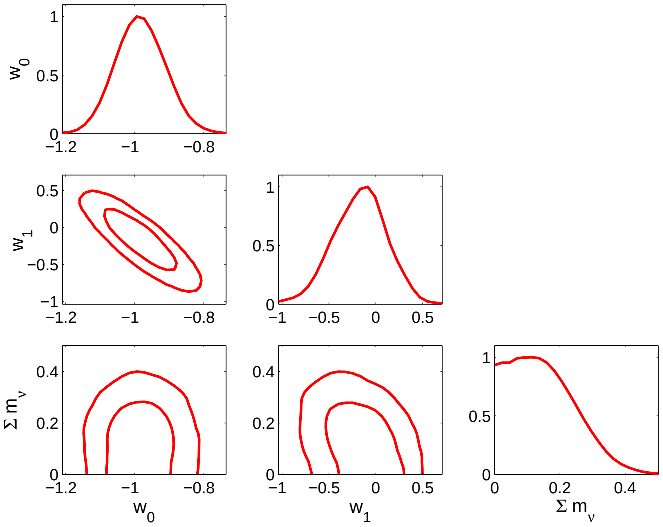

FIG. 4: Constraints on dark energy parameters w_0, w_1 and the total neutrino mass Σm_ν from the Monte Carlo method. The two dimensional contours stand for 68% and 95% confidence levels .

The reason of the correlation between Σm_ν and dark energy is not hard to understand. The main correlation between dark energy EOS and neutrino mass stems from the geometric feature of our universe[32]. In addition, dynamical dark energy will modify the time evolving potential wells which affects CMB power spectra through the late time ISW effect. Dynamical dark energy can leave imprints on CMB, LSS power spectrum and Hubble diagram nonetheless these features can be mimicked by cosmic neutrino to some extent[61]. This is the source of correlation.

IV. CONCLUSION

In this paper we have done the global fitting including parameters expressing time evolving dark energy, neutrino mass and other 6 cosmological parameters using different combination of currently data as well as simulated data for future observation. We have seen the interesting correlation between neutrino mass and EOS of time evolving dark energy especially for Σm_ν and w_1. The correlation between the "running" of dark energy EOS w_1 and the total neutrino mass Σm_ν is of great significance in determining neutrino mass limit and revealing the nature of dark energy by futuristic high precision observational data, such as SNAP, PLANCK[6] and so forth.

Acknowledgements: We acknowledge the use of the Legacy Archive for Microwave Background Data Analysis (LAMBDA). Support for LAMBDA is provided by the NASA Office of Space Science. Our MCMC chains were finished in the Shuguang 4000A system of the Shanghai Supercomputer Center(SSC). This work is supported in part by National Natural Science Foundation of China under Grant Nos. 90303004, 10533010 and 19925523. We are indebted to Patrick Mcdonald and Anze Slosar for clarifying correspondence on the fittings to the Lyman α data. We thank Antony Lewis for technical support on cosmocoffee[7]. We thank Bo Feng, Hiranya Peiris, Mingzhe Li, Pei-Hong Gu, Hong Li and Xiao-Jun Bi for helpful discussions and comments on the manuscript.

[1] D. N. Spergel *et al.*, arXiv:astro-ph/0603449.
[2] L. Page *et al.*, arXiv:astro-ph/0603450. G. Hinshaw *et al.*, arXiv:astro-ph/0603451. N. Jarosik *et al.*, arXiv:astro-ph/0603452.
[3] S. Cole *et al.* [The 2dFGRS Collaboration], Mon. Not. Roy. Astron. Soc. **362** (2005) 505
[4] M. Tegmark *et al.* [SDSS Collaboration], Astrophys. J. **606**, 702 (2004)
[5] M. Tegmark *et al.* [SDSS Collaboration], Phys. Rev. D **69**, 103501 (2004)
[6] J. L. Tonry *et al.* (Supernova Search Team Collaboration), Astrophys. J. **594**, 1 (2003).
[7] A. G. Riess *et al.* (Supernova Search Team Collaboration), Astrophys. J. **607**, 665 (2004).
[8] A. Clocchiatti *et al.* (the High Z SN Search Collaboration), Astrophys. J. **642**, 1 (2006).
[9] A.G. Riess *et al.* (Supernova Search Team Collaboration), Astron. J. **116**, 1009 (1998).
[10] S. Perlmutter *et al.* (Supernova Cosmology Project Collaboration), Astrophys. J. **517**, 565 (1999).
[11] S. Weinberg, Rev. Mod. Phys. **61**, 1 (1989).
[12] I. Zlatev, L.-M. Wang, and P. J. Steinhardt, Phys. Rev. Lett. **82**, 896 (1999).
[13] R. D. Peccei, J. Sola and C. Wetterich, Phys. Lett. B **195**, 183 (1987); C. Wetterich, Nucl. Phys. B **302**, 668 (1988); B. Ratra and P. J. E. Peebles, Phys. Rev. D **37**, 3406 (1988). P. J. E. Peebles and B. Ratra, Astrophys. J. **325**, L17 (1988).
[14] R. R. Caldwell, Phys. Lett. B **545**, 23 (2002)
[15] T. Chiba, T. Okabe and M. Yamaguchi, Phys. Rev. D **62** (2000) 023511 C. Armendariz-Picon, V. F. Mukhanov and P. J. Steinhardt, Phys. Rev. Lett. **85**, 4438 (2000)
[16] B. Feng, X. L. Wang and X. M. Zhang, Phys. Lett. B **607**, 35 (2005)
[17] B. Feng, M. Li, Y. S. Piao and X. Zhang, Phys. Lett. B **634**, 101 (2006)
[18] J.-Q. Xia, B. Feng, and X. Zhang, Mod. Phys. Lett. A **20**, 2409 (2005).
[19] G. B. Zhao, J. Q. Xia, M. Li, B. Feng and X. Zhang, Phys. Rev. D **72**, 123515 (2005).
[20] J. Q. Xia, G. B. Zhao, B. Feng, H. Li and X. Zhang, Phys. Rev. D **73**, 063521 (2006)
[21] J. Q. Xia, G. B. Zhao, B. Feng and X. Zhang, JCAP **0609**, 015 (2006).
[22] G. B. Zhao, J. Q. Xia, B. Feng and X. Zhang, arXiv:astro-ph/0603621.
[23] J. Q. Xia, G. B. Zhao, H. Li, B. Feng and X. Zhang, Phys. Rev. D **74**, 083521 (2006).
[24] M. Li, B. Feng and X. Zhang, JCAP **0512**, 002 (2005)
[25] X. F. Zhang, H. Li, Y. S. Piao and X. M. Zhang, Mod. Phys. Lett. A **21**, 231 (2006)
[26] X. F. Zhang and T. Qiu, Phys. Lett. B **642**, 187 (2006).
[27] Z. K. Guo, Y. S. Piao, X. M. Zhang and Y. Z. Zhang, Phys. Lett. B **608**, 177 (2005)
[28] For a review see E. J. Copeland, M. Sami and S. Tsujikawa, Int. J. Mod. Phys. D **15**, 1753 (2006).
[29] e.g. H. Wei and R.-G. Cai, Class. Quant. Grav. **22**, 3189 (2005); R.-G. Cai, H.-S. Zhang and A. Wang, Commun. Theor. Phys. **44**, 948 (2005); A. A. Andrianov, F. Cannata and A. Y. Kamenshchik, Phys. Rev. D **72**, 043531 (2005); X. Zhang, Int. J. Mod. Phys. D **14**, 1597 (2005); Q. Guo and R.-G. Cai, arXiv:gr-qc/0504033; B. McInnes, Nucl. Phys. B **718**, 55 (2005); I. Y. Aref'eva, A. S. Koshelev, and S. Yu. Vernov, Phys. Rev. D **72**, 064017 (2005); C. G. Huang and H. Y. Guo, arXiv:astro-ph/0508171; W. Zhao and Y. Zhang, Phys. Rev. D **73**, 123509 (2006); J. Grande, J. Sola and H. Stefancic, JCAP **0608**, 011 (2006); L. P. Chimento and R. Lazkoz, Phys. Lett. B **639**, 591 (2006); F. Cannata and A. Y. Kamenshchik, arXiv:gr-qc/0603129; R. Lazkoz and G. Leon, Phys. Lett. B **638**, 303 (2006); B. Feng, arXiv:astro-ph/0602156; H. Stefancic, J. Phys. A **39**, 6761 (2006) ; L. Perivolaropoulos, AIP Conf. Proc. **848**, 698 (2006).
[30] P. Aliani, V. Antonelli, M. Picariello and E. Torrente-Lujan, hep-ph/0309156; P. C. de Holanda and A. Y. Smirnov, Astropart. Phys. **21**, 287 (2004); M. Maltoni, T. Schwetz, M. A. Tortola and J. W. F. Valle, Phys. Rev. D **68**, 113010 (2003).
[31] W. Hu, D. J. Eisenstein and M. Tegmark, Phys. Rev. Lett. **80**, 5255 (1998).
[32] S. Hannestad, Phys. Rev. Lett. **95**, 221301 (2005).

---

[6] http://sci.esa.int/planck/
[7] http://cosmocoffee.info

[33] A. Goobar, S. Hannestad, E. Mortsell and H. Tu, JCAP **0606**, 019 (2006).
[34] E. V. Linder, Phys. Rev. Lett. **90**, 091301 (2003).
[35] A. Lewis and S. Bridle, Phys. Rev. D **66**, 103511 (2002).
[36] W. L. Freedman *et al.*, Astrophys. J. **553**, 47 (2001).
[37] S. Burles, K. M. Nollett and M. S. Turner, Astrophys. J. **552**, **L**1 (2001).
[38] H.V. Klapdor-Kleingrothaus, I.V. Krivosheina, A. Dietz, and O. Chkvorets, Phys. Lett. B **586**, 198 (2004).
[39] H.V. Klapdor-Kleingrothaus, talk at *SNOW 2006*, 2nd Scandinavian Neutrino Workshop (Stockholm, Sweden, 2006).
[40] G. L. Fogli *et al.*, hep-ph/0608060.
[41] Available from http://lambda.gsfc.nasa.gov/product/map/current/.
[42] For details see e.g. E. Di Pietro and J. F. Claeskens, Mon. Not. Roy. Astron. Soc. **341**, 1299 (2003).
[43] P. McDonald *et al.* [SDSS Collaboration], Astrophys. J. **635**, 761 (2005).
[44] D. J. Eisenstein *et al.* [SDSS Collaboration], Astrophys. J. **633**, 560 (2005).
[45] M. Tegmark *et al.* [SDSS Collaboration], Phys. Rev. D **69**, 103501 (2004).
[46] M. Cirelli and A. Strumia, JCAP **0612**, 013 (2006).
[47] A. De La Macorra, A. Melchiorri, P. Serra and R. Bean, arXiv:astro-ph/0608351.
[48] A. Lewis, Phys. Rev. D **71**, 083008 (2005).
[49] R. Easther, W. H. Kinney and H. Peiris, JCAP **0505**, 009 (2005).
[50] L. Perotto, J. Lesgourgues, S. Hannestad, H. Tu and Y. Y. Y. Wong, JCAP **0610**, 013 (2006).
[51] Available at http://www.lamost.org/.
[52] H. A. Feldman, N. Kaiser and J. A. Peacock, Astrophys. J. **426**, 23 (1994).
[53] Available at http://snap.lbl.gov/.
[54] A. G. Kim, E. V. Linder, R. Miquel and N. Mostek, Mon. Not. Roy. Astron. Soc. **347**, 909 (2004).
[55] H. Li, B. Feng, J. Q. Xia and X. Zhang, Phys. Rev. D **73**, 103503 (2006).
[56] A. Gelman and D. Rubin, Statistical Science **7**, 457 (1992).
[57] C. -P. Ma and E. Berschinger, Astrophys. J. **455**, 7 (1995).
[58] Bhattacharyya,G.K. and R.A.Johnson, *Statistical Concepts and Methods.* New York: John Wiley, 1977.
[59] e.g. L. M. Wang, R. R. Caldwell, J. P. Ostriker and P. J. Steinhardt, Astrophys. J. **530**, 17 (2000).
[60] K. Ichikawa and T. Takahashi, arXiv:astro-ph/0510849.
[61] P. S. Corasaniti, B. A. Bassett, C. Ungarelli and E. J. Copeland, Phys. Rev. Lett. **90**, 091303 (2003).